Int. J. Electrochem. Sci., 16 **(2021)** Article Number: 211135, doi: 10.20964/2021.11.51

International Journal of
ELECTROCHEMICAL
SCIENCE
www.electrochemsci.org

Inhibitor Effect of N-(5-((4-chlorophenyl)diazenyl)-2-hydroxy benzylidene)-2-hydroxy benzohydrazide for Mild Steel Corrosion in chloride and sulphate acidic solutions

G. Pandimuthu[1,2], K.Muthupandi[3], Tse-Wei Chen[4,5], Shen-Ming Chen[4,], A.Sankar[1,*], P. Muthukrishnan[6], Syang-Peng Rwei[5,7]*

[1] Department of Chemistry, Kandaswami Kandar's College, P.Velur, Namakkal-638 182, India.
[2] Department of Chemistry, Arumugam Pillai Seethai Ammal College, Tiruppatur-630211, India.
[3] Department of Chemistry, Mannar Thirumalai Naicker College, Madurai-625004, India.
[4] Electroanalysis and Bioelectrochemistry Lab, Department of Chemical Engineering and Biotechnology, National Taipei University of Technology, No. 1, Section 3, Chung-Hsiao East Road, Taipei 106, Taiwan, ROC.
[5] Research and Development Center for Smart Textile Technology, National Taipei University of Technology, Taipei 106, Taiwan, ROC
[6] Department of Chemistry, Faculty of Engineering, Karpagam Academy of Higher Education, Coimbatore-641021, India.
[7] Institute of Organic and Polymeric Materials, National Taipei University of Technology, Taiwan
[*]E-mail: smchen78@ms15.hinet.net, sanvishnu2010@gmail.com

Received: 2 August 2021 / *Accepted:* 17 September 2021 / *Published:* 10 October 2021

Corrosion resistance of N-(5-((4-chlorophenyl)diazenyl)-2-hydroxybenzylidene)-2-hydroxybenzo hydrazide (CDHBHZ) in reducing mild steel (MS) corrosion in 1M hydrochloric acid (HCl) and 0.5M sulphuric acid (H_2SO_4) were examined by Electrochemical and Chemical techniques. The results from mass loss analysis revealed that the corrosion rate of MS enhanced when the temperature was raised from 308K to 328K. It is noted that in the acidic solutions, the dissolution rate of MS reduced with raise in the concentration of CDHBHZ (0.01- 0.03M) and it resulted in higher inhibition rate in HCl than H_2SO_4 solution. The diameter of the semicircle increased as the amount of CDHBHZ increased, as shown by the Nyquist plots. The protection efficacy of CDHBHZ was 96.00 % (1M HCl) and 89.00% (0.5 H_2SO_4) at the ideal CDHBHZ concentrations. CDHBHZ functions as a comprehensive inhibitor that predominantly inhibit corrosion at anodic site, according to Polarization studies. The IR spectroscopic analysis confirms the functional groups in the CDHBHZ and the formation of inactive thin films on MS surface. The adsorption of CDHBHZ on the MS follows Langmuir model, according to Thermodynamic and adsorption studies.

Keywords: Alloys, Hydrazone, Corrosion reduction rate, Chemical analysis, Langmuir model.

1. INTRODUCTION

Organic compounds are utilized as acid corrosion inhibitors in a number of industrial uses including preventing the metal dissolution, reducing the undesirable destructive effect, and acid treatment solutions [1]. In industry, the majority of effective compounds are organic inhibitors which usually comprise with heteroatoms (inclusive of S, N and O) and many linkages in the inhibitor molecules that adsorb over the metal floor. A review of the literature found that a vast variety of organic compounds [2-6] studied and assessed as acid inhibitors. For organic inhibitors, the strength of the adsorption bond is the most important aspect and its efficiency is determined by the chemical structure, chemical composition and affinity [7]. Despite the huge number of synthetic organic inhibitors available, the options for choosing a suitable inhibitor for a specific system are restricted due to inhibitor specificity and the wide range of corrosion systems [8]. Some hydrazide and hydrazones have recently been suggested to be efficient anti corrosion agents for copper [9], and lead [10] in acidic conditions. The use of CDHBHZ as a corrosion inhibitor has not been investigated in the literature. The inhibitor is chosen based on the following information.

Inhibitors have two kind of heteroatoms (like O and N in CDHBHZ), which play crucial role in the adsorption process and metal surface interaction. Inhibitors dissolve easily in testing solution. Inhibitors do not pose any health risks, unlike other sulfur-containing compounds; hence CDHBHZ can be used as a corrosion inhibitor with confidence. CDHBHZ preparation processes that are relatively affordable.Various methodologies were used to study the inhibiting action of N-(5-((4-chloro phenyl) diazenyl)-2-hydroxy benzylidene)-2-hydroxy benzohydrazide (CDHBHZ) on mild steel (MS) corrosion in solution (1M HCl and 0.5M H_2SO_4) was examined.

2. MATERIALS AND METHODS

2.1. Materials

Chemical analysis was carried out using mild steel specimens with diameters of 2.5 ×1.0 × 0.1 cm with a necessary composition of 0.032% Mn, 0.029% S, 0.092% C and 99.847% Fe. The working electrode was made from mild steel rod and then coated with araldite to give it a 0.2826cm^2 exposed area. Prior doing all experiments, MS is abraded with abrasive papers upto 4/0 grades. After abrading, the specimens scoured and cleaned with ethanol, dried at ambient temperature. Solutions (HCl 1M & H_2SO_4 0.5M) were prepared from AR grade of HCl & H_2SO_4 using deionized water. CDHBHZ was synthesized by refluxing a mixture of 5-((4-chlorophenyl)diazenyl)-2-hydroxybenzaldehyde and 2-hydroxybenzohydrazide (1:1 molar ratio) in ethanol for 2 hours. After allowing the solution to cool to ambient temperature, the yield was filtered, rinsed with alcohol and dried [11]. The systematic scheme of the synthesized CDHBHZ is presented in Fig.1.

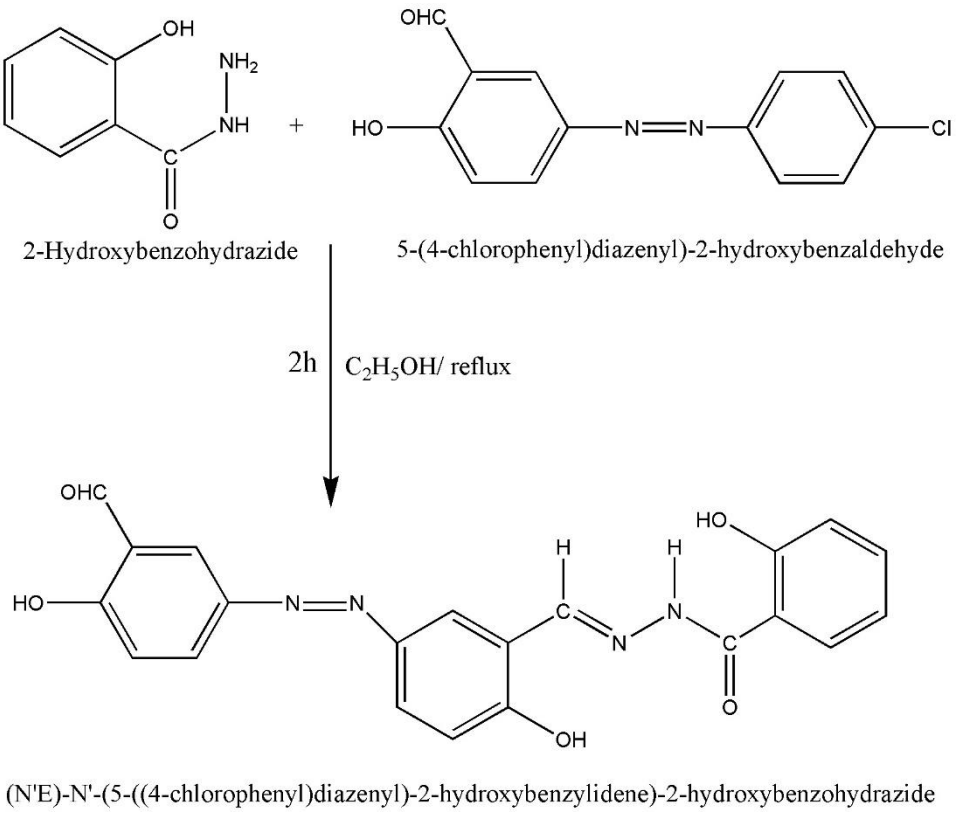

Figure 1. The route for CDHBHZ synthesis

2.2. Preliminary Corrosion assessment (Chemical Analysis)

Corrosion behaviors of MS in both solution (1M HCl & 0.5 M H_2SO_4) were examined by mass loss measurements. In this study, MS specimens (three sets) were soaked in 100 ml of test solution for 2 h at different temperatures (308-328K) in the presence and absence of CDHBHZ. The specimens are taken from solution after 2h, rinsed with deionized water, thoroughly dried and weighed. The weight loss of MS before and after immersion is measured utilizing electronic weighing balance with a 0.1 mg precision. Three times the experiments are executed, with the weight losses averaging out. The corrosion rate (Cr) and protection efficiency (PE %) are determined using Eq (1) & (2):

$$Cr\ (mpy) = 534 \times LM_b\text{-}LM_a\ /DST \quad (1)$$

$$PE\ \% = (LM_0 - LM_i) / LM_0 \times 100 \quad (2)$$

Where LM_b and LM_a refers to the average mass of MS prior and after dipped in both test solution. LM_0 and LM_i indicates the mass loss of MS in the absence and presence of CDHBHZ respectively, D is the mild steel density, S is the area of the specimen in cm^2, T is the duration of specimen exposure in hours.

2.3. Determination of Electrochemical parameters

AC impedance and Potentiodynamic polarization experiments were carried out utilizing Electrochemical analyzer (CH instruments-Model 604D) by connecting the three electrode cell that

included a Pt foil as a auxiliary electrode, calomel electrodes as the standard electrode and MS as the working electrode (0.2826cm^2 exposed area). All electrochemical experiments were done in steady state at 308K with 100ml of electrolyte (1M HCl and 0.5M H_2SO_4) in steady state. In order to achieve a stable potentials, the working electrode is dipped in 100ml of aggressive solution for ½ hour. Potentiodynamic polarisation curves were recorded from -300 to + 300 mV at 0.001 V/sec. AC impedance measurements were carried out in the frequency range of 0.1Hz to 100 KHz with amplitude of 5mV. This experiment is carried out thrice to ascertain reproducibility of the electrochemical data. The maximum frequency (f_{max}) and the solution resistance (S_R) values were obtained from Nyquist plot. The following equation is employed to compute the double layer capacitance (DL_c) and charge transfer resistance (CT_R) values:

$$CT_R = (S_R + CT_R) - S_R \quad (3)$$

$$DL_c = ½\pi \times CT_R \times f_{max} \quad (4)$$

2.4. Analysis of Functional groups

The IR spectra of CDHBHZ and the rubbed rust sample of the absorbed layer created on the surface of MS after exposure to 0.03M CDHBHZ in 1M HCl and 0.5 H_2SO_4 were recorded using Shimadzu FT-IR spectrophotometer (Model 8400S) with a range of 4 to 40m^{-1} and KBR disk approach.

2.5. Scanning Electron Microscopic (SEM) Techniques

Immersing the MS specimens in HCl and H_2SO_4 solutions alone and with 0.03M CDHBHZ for 2 hours, they are brought out the test solution and dried. After drying them, the nature of the protective film generated on the surface of the MS is analyzed using JEOL JSM 6390 (SEM).

3. RESULTS AND DISCUSSION

3.1. Effect of CDHBHZ concentration and Temperature by Mass Loss analysis

Fig.2a and b show the corrosion rate (C_r) and protection efficiency (% PE) of MS exposed to 0.5 M H_2SO_4 and 1 M HCl alone and with divergent amount of CDHBHZ. According to findings, CDHBHZ reduces mild steel corrosion and enhances % PE in both acid conditions. This means that the adsorption of CDHBHZ increases the MS surface coverage [12]. Both aggressive solutions showed greatest protection efficacy (96% in HCl and 89% in H_2SO_4) at 0.03M CDHBHZ concentration and 308K. Above 0.03M, the corrosion rate and protection efficiency in both solution remain unchanged. A comparison of the anticorrosive behavior of different organic inhibitors finds that CDHBHZ shows more efficacy than others [13-16]. Figure 2 demonstrates that the protection efficiency reduced with increase of temperatures, owing to increasing MS dissolution rates and the enhanced desorption of CDHBHZ from the MS surface at 328K [17,18]. Inspection of the figure 2, it is noted that protection efficacy of CDHBHZ in HCl is greater than in H_2SO_4. This higher efficacy may be due to the greater surface coverage from HCl because of stronger adsorption of the chloride ions on the MS surface [19].

In the present investigation, highest protection efficiency (96% in HCl and 89% in H_2SO_4) of CDHBHZ was observed at 303K and further temperature increases resulted in a substantial drop in surface coverage [20]. Several researchers have made similar observations [21-23].

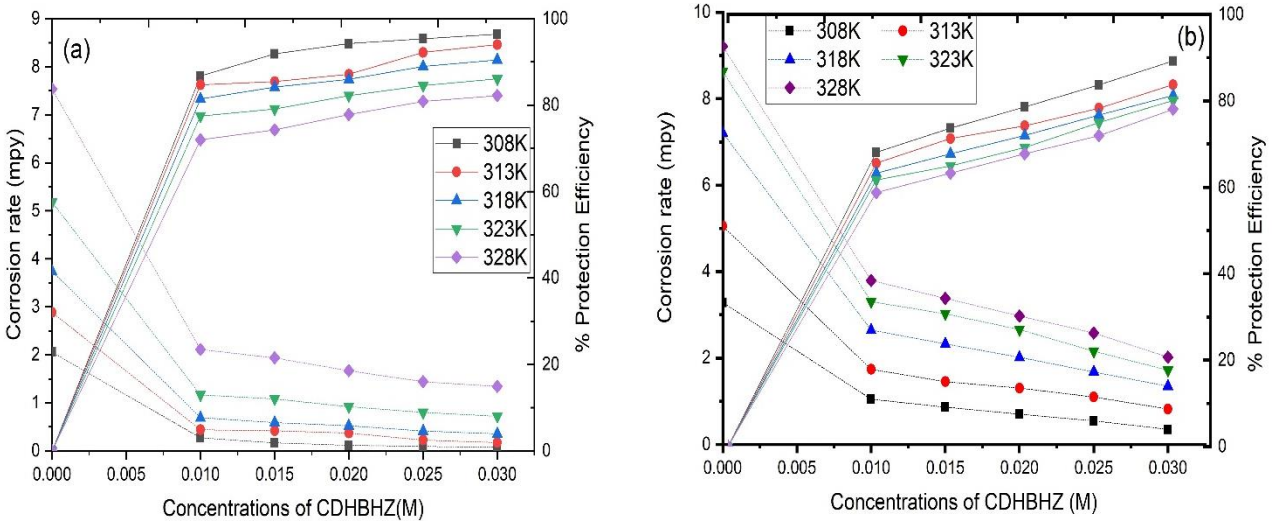

Figure 2. Effect of CDHBHZ on Corrosion rate (---) and % PE (-) of CDHBHZ on MS in HCl (a) and H_2SO_4 (b) at 308-328K.

The inhibited acid metal reaction is greatly influenced by temperature and its complicated because several changes occur on the metal surface like inhibitor peeling, decomposition and fast etching [24]. The Arrhenius equation can be used to express the interrelation between corrosion rate (C_r) and absolute temperature (T)

$$\log Cr = -(E_a/2.303RT) + \log A \quad (5)$$

Here, pre-exponential constant is designated by A, E_a indicates the activation energy and R is the molar gas constant. Arrhenius plots of MS in acid solution alone and with divergent amount of CDHBHZ are depicted in Fig. 3a & b. From the plots of log Cr against 1/T, the values of E_a collected from the slopes and are displayed in Table 1. Data in Table 1 explain that the E_a values in the presence of CDHBHZ ranged from 43.85 to 71.40 kJ/mol (0.5 M H_2SO_4) and 53.40 to 121.55 kJ mol^{-1} (0.5M HCl). The values of E_a in the presence of CDHBHZ is greater than the absence of CDHBHZ (Table 1). This is because the energy barrier of the corrosion reaction rises as the concentration of CDHBHZ rises. Furthermore, the physical adsorption mechanism is thought to be obeyed when the E_a is between 40 - 80 kJ mol^{-1} [25, 26].

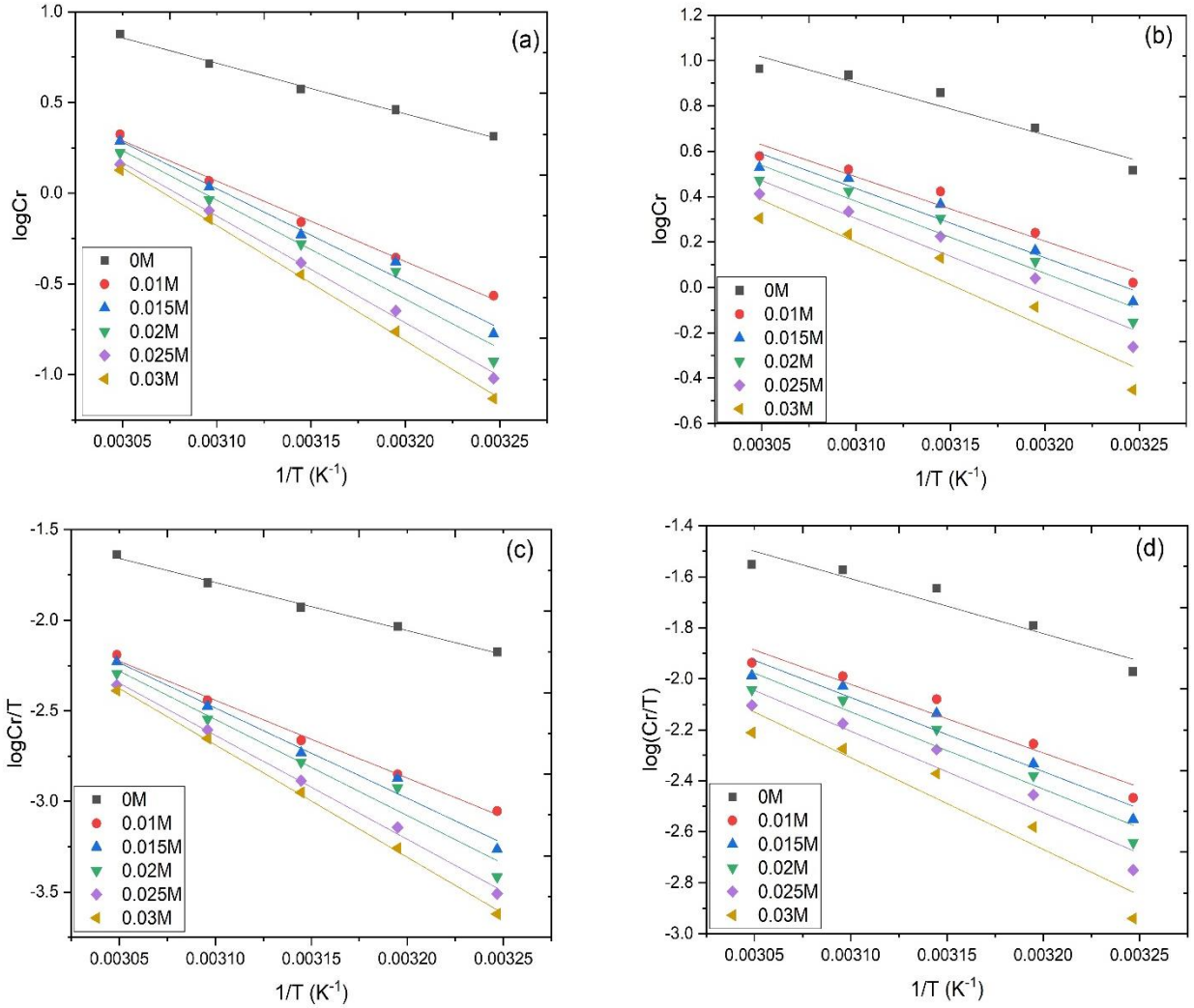

Figure 3. The plot of log Corrosion rate vs 1/T for MS in HCl (a) and H_2SO_4 (b) with and without CDHBHZ and log Corrosion rate/T vs 1/T for MS in HCl (c) and H_2SO_4 (d) with and without CDHBHZ.

This theory is supported by the fact that protection efficiency decreases as temperature rises. Only E_a can choose the adsorption mode since there is rivalry for adsorption on the metal surface between water and inhibitor molecules, and removing water molecules from the surface demands some activation energy [27]. As a result, both chemical and physical mechanisms are involved in the adsorption of CDHBHZ on the MS surface in both solution [28]. The transition state equation is as follows

$$\log Cr/T = \{- (\Delta H^*/ 2.303RT) - (\log(R/hN) + (\Delta S^*/2.303R)\} \quad (6)$$

Here, Plank's constant denoted h, Avogadro's number denoted R, ΔS refers to the entropy of activation and ΔH indicates enthalpy activation. The values of ΔS* and ΔH* were calculated with an intercept of [log (R/Nh) + (ΔS*/2.303R)] and slope of (ΔH*/2.303R) (Fig.3c& d) and compiled in Table 1. The positive value of enthalpies reflects the endothermic nature of the steel dissolving process, indicating that the MS dissolution is very slow. In 1M HCl, the ΔS* values increased positively in inhibited solution than non-inhibited solution. In 1M HCl with different concentrations of CDHBHZ, ΔS* was found to be positive, whereas in 1M HCl, it was shown to be negative. This shows

that the system is transitioning from less orderly to a more random arrangement [29]. The values of ΔS^* in 0.5M H_2SO_4 and inhibited solutions were negative, this shows that the transition state in the rate-limiting step indicates an association rather than a dissociation phase, implying that disordering diminishes as one moves from reactants to the activated complex [30, 31].

Table 1. Thermodynamic properties of MS without and with different CDHBHZ concentrations.

Test solutions	Concentrations of CDHBHZ (M)	E_a (kJ/mol)	ΔH_a (kJ/mol)	ΔS_a (J/mol/K)
1M HCl	0	53.40	50.77	-74.48
	0.01	85.06	82.42	7.34
	0.015	98.21	95.57	51.15
	0.02	104.44	101.80	69.26
	0.025	112.69	110.04	93.13
	0.03	121.55	118.91	119.61
0.5M H_2SO_4	0	43.85	41.20	-100.59
	0.01	54.22	51.58	-76.35
	0.015	58.40	55.76	-64.42
	0.02	60.75	58.11	-58.20
	0.025	63.84	61.19	-50.04
	0.03	71.40	68.76	-28.62

3.2. Adsorption Isotherms

The inhibitor effect of organic molecules on electrode surface is measured using adsorption isotherms. Organic corrosion inhibitors protect metal from corroding by adsorbing to the metal surface and generating an insulated layer. Experimental data from the chemical analysis was graphically evaluated to fit different isotherms such as the Temkin, Frumkin and Langmuir adsorption models. The obtained data is well fitted with the Langmuir model. A plot of C (g/l) against C/ θ for CDHBHZ yield straight line (Fig.4a &b). According to the plots, the adsorption of CDHBHZ on electrode surface in 1M solution (HCl and H_2SO_4) followed the Langmuir adsorption model.

$$C/\theta = C + 1/K_{ads} \quad (7)$$

Here C is the inhibitor concentrations, K_{ads} represents the adsorption constant and θ is the surface coverage. The values of K_{ads} were determined from the intercept of the straight lines and compiled in table 2. The following equation connects the standard free energy of inhibitor adsorption (ΔG_{ads}) and the adsorption constant (K_{ads})

$$\Delta G_{ads} = -RT \ln (55.5 \times K_{ads}) \quad (8)$$

Here, Temperature is T and the concentration of water is 55.5 M. When rising temperature, the values of K_{ads} decreased, indicating that the attractions that takes place between the MS and adsorbed molecules are feeble and the CDHBHZ molecules are more quickly removed. These findings showed that the protective efficacy diminishes as the temperature enhances. Physical adsorption is indicated by the values of ΔG_{ads} less than −20 kJ/mol, which are commensurate with the van der Waals interaction that takes place between the charged electrode and inhibitor that are also charged. Chemisorption,

which involves the a pair of valence electron or pi- electrons in organic molecules that are shared or transferred with the electrode surface and establish a dative bond, is associated with values about - 40 kJ/mol or higher [32]. In this study, the obtained ΔG_{ads} values are −23.85 and −27.97 kJ/mol (between -20kJ/mol and -40kJ/mol) for CDHBHZ. The negative values of ΔG_{ads} clearly show that the adsorption of CDHBHZ on MS surface occurs spontaneously via comprehensive adsorption mechanism [33]. The standard enthalpy of adsorption (ΔH_{ads}) and entropy of adsorption (ΔS_{ads}) are crucial metrics for understanding adsorption behavior of inhibitors on metal surface. The van't Hoff equation is used to compute the enthalpy of adsorption (ΔH_{ads}):

$$\ln K_{ads} = -\Delta H_{ads} / RT + \text{constant} \quad (9)$$

Fig 5 depicts the straight lines of the plot of ln K_{ads} vs 1/T, with slope is equal to $-\Delta H_{ads}/R$. The ΔS_{ads} can be obtained by the thermodynamic equation:

$$\Delta S_{ads} = \frac{\Delta H_{ads} - \Delta G_{ads}}{T} \quad (10)$$

The values of ΔH_{ads} were estimated to be -37.06 and -14.33 kJ/mol for CDHBHZ in both solution, respectively. The negative values of ΔH_{ads} suggest that the adsorption of CDHBHZ is an exothermic type, implying lower protection efficacy at 328K. This shows the progressive removal of CDHBHZ from the surface of MS [17]. The absolute value of ΔH_{ads} is used to distinguish physisorption from chemisorption in an exothermic process. The values of ΔH_{ads} for physisorption is less than 40kJ/mol, but it exceeds 100 $kJmol^{-1}$ for chemisorption [34]. In this work, ΔH_{ads} values are lower than physical adsorption heat, once again suggesting that the adsorption of CDHBHZ on MS surfaces is mostly physisorption. In both acid solution, the values of ΔS_{ads} are closely constant, and they are negative. There are two possible explanations for this behavior [35**,** 36]; (i) Prior the adsorption process, inhibitors can easily migrate in the test solution implying that inhibitor molecules are chaotic. (ii) During the adsorption process, inhibitors are orderly adsorbed onto the steel surface, resulting in a decrease in entropy.

Table 2. Langmuir model for MS without and with different CDHBHZ concentrations.

Test solutions	Temperature (K)	K_{ads} (L/mol)	$-\Delta G_{ads}$ (kJ/mol)	ΔH_{ads} (kJ/mol)	$-\Delta S_{ads}$ (J/mol/K)	R^2
1M HCl	308	1000	27.97		29.51	1.000
	313	500	26.62		33.35	0.996
	318	500	27.05	-37.06	31.48	0.999
	323	500	27.47		29.69	0.999
	328	333.33	26.79		31.31	0.998
0.5M H_2SO_4	308	200	23.85		30.90	0.993
	313	200	24.24	-14.33	31.66	0.993
	318	166.67	24.14		30.84	0.993
	323	166.67	24.52		31.55	0.990
	328	142.86	23.95		28.02	0.989

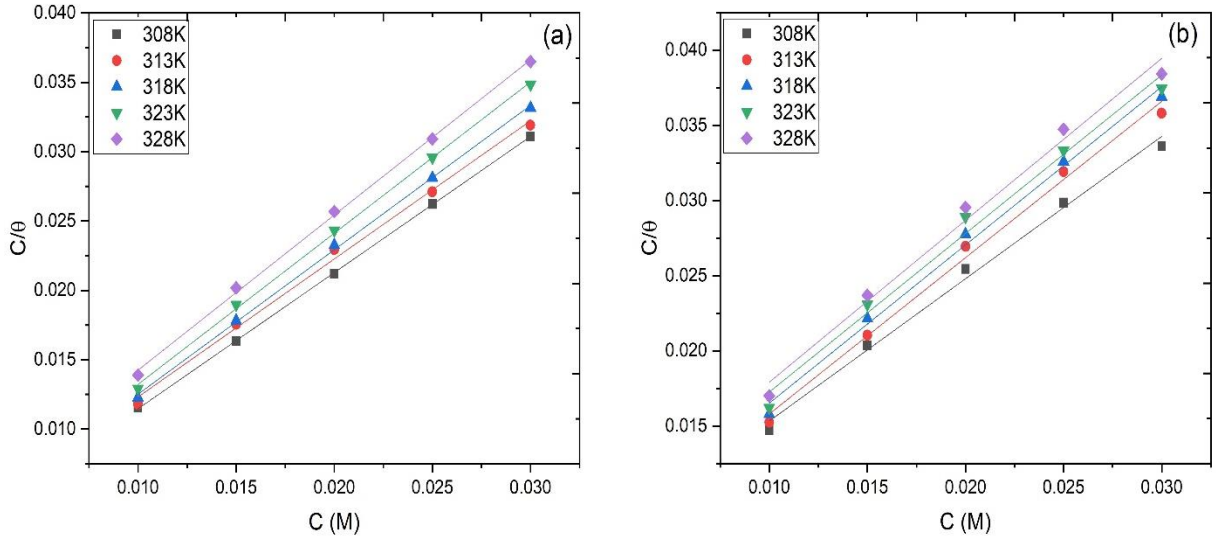

Figure 4. The plots between C/θ and C for CDHBHZ on MS in HCl (a) and H_2SO_4 (b) at 308-328K.

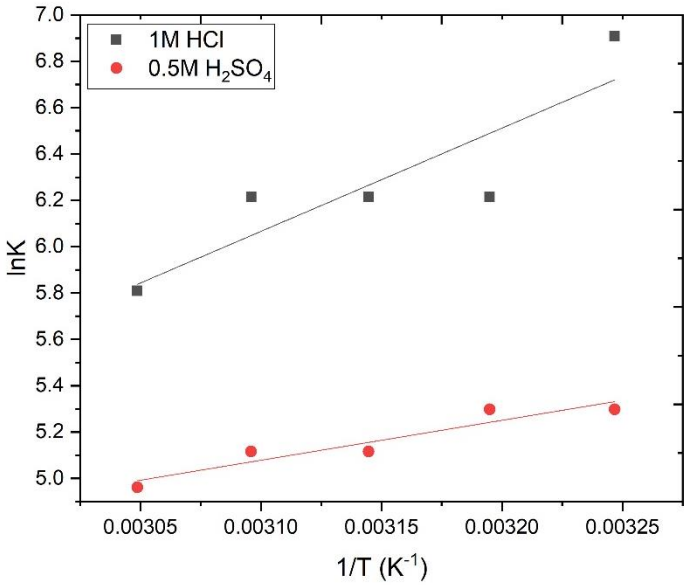

Figure 5. The plots of ln K_{ads} vs 1/T for CDHBHZ on MS in HCl and H_2SO_4.

3.3. Potentiodynamic Polarization studies

Potentiodynamic Polarization were performed to evaluate the influence of CDHBHZ on the cathodic and anodic region of metal surface. Table 3 lists the polarization parameters that were investigated, including corrosion potential (E_{corr}), anodic slope (β_a), cathodic slope (β_c) and current density (I_{corr}). The table clearly reveals that when CDHBHZ concentrations (0.01 – 0.03M) are increased, the I_{corr} values decrease and PE increases considerably. Tebbji et al [37] reported similar effect when BBPA was employed as an inhibitor**.** At 0.0005M of BBPA in 1 M HCl, they discovered that the maximum protection efficacy was 83.79%. In this work, the highest protection efficacy of 83.47%, 91.75% could be with 0.03M of CDHBHZ in H_2SO_4 and HCl respectively. P. Mourya et.al [38] reported highest efficiacy of 96.68% and 96.2.3% with 450×10^{-6}M of 4-(N,N-dimethylamino)

benzaldehyde thiosemicarbazone in 0.5 M H_2SO_4 and 1 M HCl. The anodic and cathodic plots of MS immersed in without (HCl & H_2SO_4) and with various concentrations of CDHBHZ at 308K are displayed in Fig. 6a & b. The addition of CDHBHZ into 1 M HCl changes E_{corr} towards the anodic site and reduces the corrosion on anodic and cathodic sites of MS, as shown in Fig.6a. This shows that CDHBHZ controlled corrosion on anodic sites significantly and cathodic sites on the electrode surface. In 0.5 M H_2SO_4 solution, E_{corr} also shifts to positive, indicating that CDHBHZ may be organized as an anodic inhibitor with CDHBHZ molecules more adsorbed on the anodic region, inhibiting anodic reactions.

Table 3. Potentiodynamic Polarization of MS in the presence of CDHBHZ in both acid solutions.

Test solutions	C_{inh}(M)	$-E_{corr}$ (mV)	j_{corr} (mA cm^{-2})	$-\beta_c$ (mV/decade)	$-\beta_a$ (mV/decade)	% PE
1M HCl	0	451	5.700	183	173	-
	0.01	436	1.672	180	129	70.66
	0.015	433	1.395	176	126	75.52
	0.02	442	1.041	226	105	81.73
	0.025	439	0.725	219	106	87.28
	0.03	443	0.470	210	101	91.75
0.5M H_2SO_4	0	448	6.238	173	157	-
	0.01	451	1.921	199	119	69.20
	0.015	444	1.598	210	119	74.38
	0.02	442	1.530	201	136	75.47
	0.025	446	1.048	207	129	83.19
	0.03	451	1.031	199	104	83.47

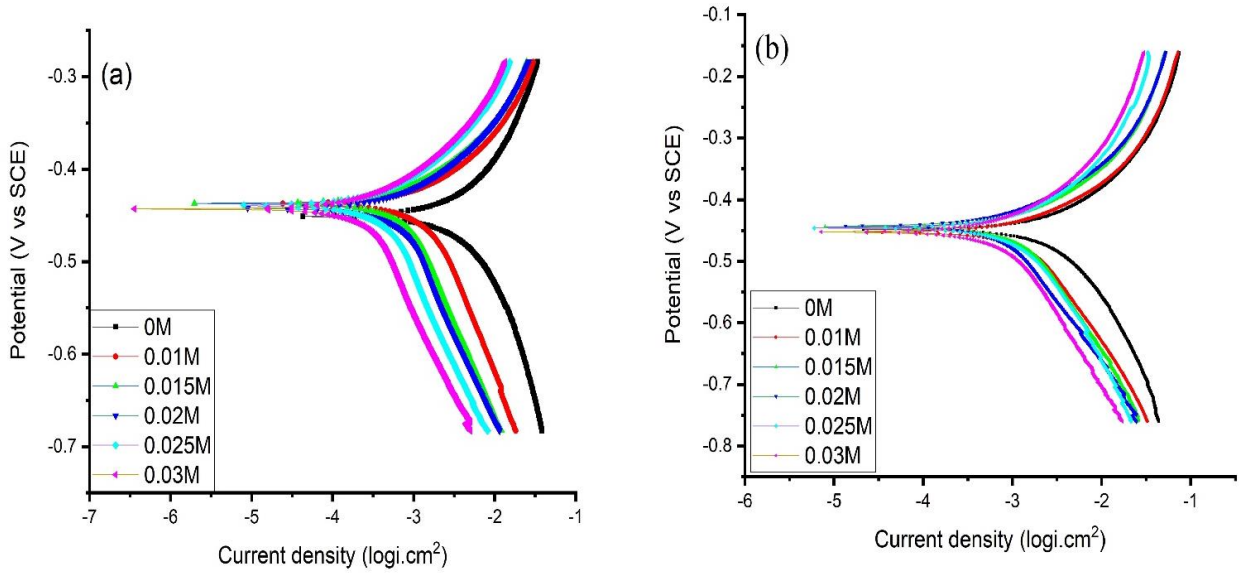

Figure 6. Potentiodynamic polarization curves of MS in the presence of CDHBHZ in HCl (a) and H_2SO_4 (b) at 308K.

Data in Table 3 indicate that there was no discernible direction in the shift of E_{corr} values, in the presence of CDHBHZ in 0.5 M H_2SO_4 and HCl media. In both media, this finding revealed that CDHBHZ can be characterized as a comprehensive inhibitor in both solutions. Table 3 further demonstrates that at individual CDHBHZ concentration, I_{corr} (0.5 M H_2SO_4) > I_{corr} (1 M HCl); whereas % PE (1 M HCl) > % PE (0.5 M H_2SO_4). According to the findings of this study, Fe is quickly soluble in aggressive media at very low inhibitor concentrations, which speeds up the corrosion reaction. As the CDHBHZ concentration rises, more CDHBHZ molecules are deposited on the MS surface, reducing the dissolution rate of mild steel [39].

3.4. AC Impedance study

Impedance plots for MS in acid and inhibited solutions are displayed in Fig.7a and b. The diameters of the capacitive loops with the addition of CDHBHZ to the aggressive solution, indicating, a single capacitive loop in both solution due to charge transfer processes. The strengthening of the inhibitor layer is indicated by the rise in the diameter of Impedance curves as the concentration of CDHBHZ increases [40]. Table 4 shows the electrochemical parameters acquired from Impedance curves such as S_R, CT_R and DL_c values. As indicated in the table, the CT_R increases as the CDHBHZ concentration increases in both solution, showing the existence of an insulated film on MS surface [41]. In the impedance studies, PE% is calculated as:

$$PE\% = (CT_R - CT^0_R / CT_R) \times 100 \quad (11)$$

Here CT^0_R and CT_R are charge transfer resistance in the presence and absence of inhibitor respectively**.** Table 4 clearly shows that after addition of CDHBHZ concentrations, CT_R values increase and DL_c decreases. The decrease in DL_c is caused by the continuous replacement of water molecules by the adsorption of CDHBHZ that takes place between electrode/electrolyte interface, causes a protective coating to develop on the MS surface, which then slows the dissolution of Fe. The decrease in DL_c has been associated to an increase in electrical double layer thickness [42, 43]. These findings indicate that CDHBHZ significantly adsorbs on the surface of MS. The maximum protection efficiency (86.99% for 1 M HCl and 86.31% for 0.5 M H_2SO_4) was achieved at 0.03M of CDHBHZ. The high PE% is due to the presence of additional pi-electrons, N and O atoms in its chemical structure. Table 5 shows the percentage protection efficiency and optimum concentrations of some organic products employed as an inhibitor in different aggressive medium.

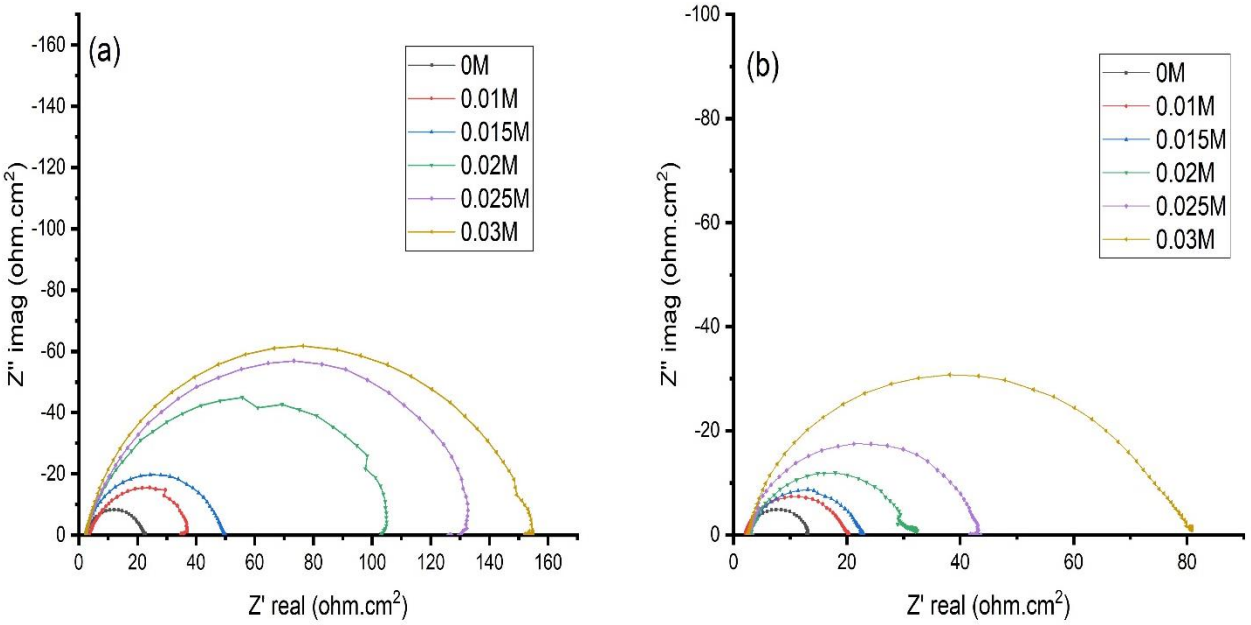

Figure 7. Nyquist curves for MS in HCl (a) and H_2SO_4 (b) with and without CDHBHZ at 308K.

Table 4. Electrochemical data for MS in the presence and absence of CDHBHZ.

Test solutions	C_{inh}(M)	S_R (Ωcm^2)	CT_R (Ωcm^2)	DL_c (F/cm^2)	% PE
1M HCl	0	2.550	19.65	9.45×10^{-4}	-
	0.01	3.610	31.35	2.63×10^{-4}	37.32
	0.015	2.598	46.95	1.70×10^{-4}	58.15
	0.02	2.397	94.17	3.32×10^{-5}	79.13
	0.025	2.431	119.47	2.09×10^{-5}	83.55
	0.03	2.507	151.06	1.66×10^{-5}	86.99
0.5M H_2SO_4	0	2.245	10.66	2.94×10^{-3}	-
	0.01	2.128	16.44	1.81×10^{-3}	35.15
	0.015	2.733	19.73	1.62×10^{-3}	45.97
	0.02	3.239	27.79	4.81×10^{-4}	61.64
	0.025	2.702	39.04	2.64×10^{-4}	72.69
	0.03	2.537	77.88	6.72×10^{-5}	86.31

The results obtained by a large number of organic compounds (Table 5) and our findings (Table 3 and 4) indicate that the CDHBHZ could be effective corrosion inhibitors. The protection efficiency for CDHBHZ at a concentration of 0.03M CDHBHZ is depicted in Fig.8 employing three diverse techniques namely mass loss, polarization and EIS. The results of the chemical and electrochemical studies are all consistent.

Table 5. Percentage protection efficacy of various synthetic inhibitors at ideal concentration in acid media.

Synthetic inhibitors	Metal exposed	Optimum concentration	Acidic media	Techniques (Highest Protection efficiency)		
				Mass loss	Polarization	Impedance
N-((1H-pyrrol-2-yl)methylene) nicotinamide [44]	Mild steel	500ppm	0.5M HCl	80.60	83.80	83.00
N-((methyl-(phenyl)amino)methylene) nicotinamide [44]	Mild steel	500ppm	0.5M HCl	86.30	86.6	85.40
N,N -bis(salicylidene)-2-hydroxy-1,3-propanediamine [45]	Mild steel	0.005M	2M HCl	79.00	78.0	80.00
N-[(3,4-dimethoxyphenyl) methyleneamino]- 4-hydroxy-benzamide [46]	Mild steel	0.003M	0.5M H_2SO_4	-	86.00	82.34
			0.5M HCl		81.57	75.98
1- [morpholin-4-yl(thiophen-2-yl)methyl]thiourea [47]	Mild steel	500ppm	0.5M HCl	-	86.27	83.81
2-chloro 3-formyl quinoline [48]	Mild steel	200ppm	1M HCl	88.22	85.03	85.34
3a,6a-diphenyltetrahydro-1H-imidazo [4,5-c] [1, 2, 5] thiadiazole-5(3H)-thione 2,2-dioxide [49]	Mild steel	120µM	0.5M H_2SO_4	93.4	80.4	92.0
triethylene tetramine [50]	Mild steel	0.01M	1M HCl	79.7	84.00	85.00
hexamethylene tetramine [50]	Mild steel	0.01M	1M HCl	88.6	90.40	93.00
N'furan-2-yl-methylene-hydrazine carbodithioic acid [51]	Mild steel	0.001M	0.5 M HCl	85	91.65	80.3
In this work: CDHBHZ	Mild steel	0.03M	1M HCl	96.00	91.75	86.99
	Mild steel	0.03M	0.5M H_2SO_4	89.00	83.47	86.31

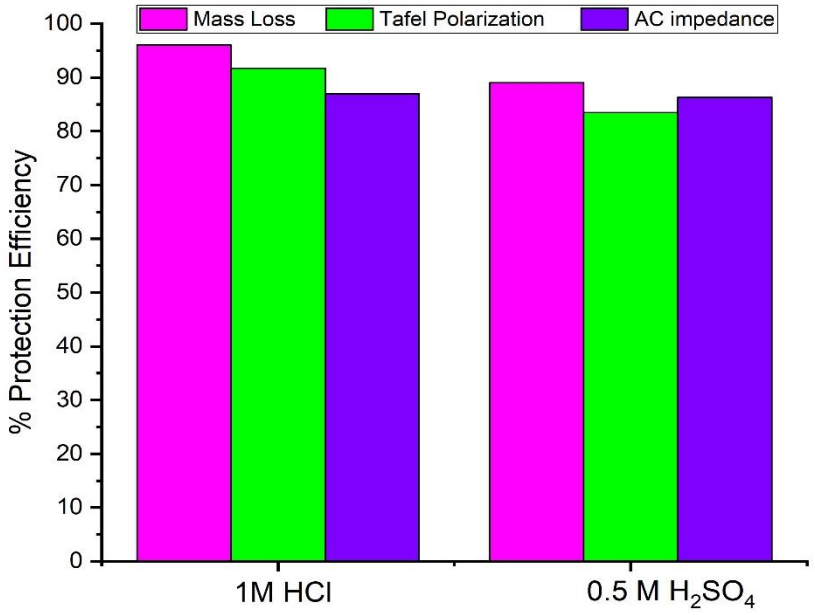

Figure 8. Comparison of % PE using mass loss, Potentiodynamic and AC impedance analysis

3.5. Influence of functional groups on mild steel protection

The obtained IR spectra of CDHBHZ is displayed in Fig.9a. The presence of a hydrogen bond is shown by the original band at 3421 cm^{-1}. This band confirms existence of O-H groups. The wave numbers at 3159 cm^{-1} and 3049 cm^{-1}, describing N-H and C-H stretching with aromatic ring. Carbonyl stretching vibrations with aromatic ring are attributed to the sharp peak at 1610 cm^{-1} in the CDHBHZ. At 1145 cm^{-1} and 1313 cm^{-1}, there are two peaks for C-N stretching of aromatic ring. The bending vibrations of -CH_2 are represented by the band at 1427 cm^{-1}. The band at 765 cm^{-1} is caused by C-H bending vibration in benzene. Figure.9b & c show the IR spectrum of scrapped samples formed on MS surfaces exposed to in HCl (1M) and 0.5M H_2SO_4 with presence of CDHBHZ. All major peaks in CDHBHZ emerge in barrier layer on the MS surface, as shown in figure 9b & c. The C-H symmetric and asymmetric aliphatic stretching vibrations are noticed at 2924, 2854 and 2972cm^{-1}. Furthermore, the adsorption mode at 2343cm^{-1} noted in Figure 9b, is attributed to NH^+ stretching vibration. This indicates that a protonated form of CDHBHZ or nitrogen atoms adsorbed on the MS surface. The stretching frequencies of a broad bands at 3388 and 3414cm^{-1}, indicating that the inhibited layer contains water. In acid solutions, the disappearance of N-H stretching (from 3000 to 3300 cm^{-1}) is caused by protonated CDHBHZ. Due to interaction of π-electrons of aromatic ring with metal, the peak (N-H stretching) at 1529 cm^{-1} disappeared. Inspection of FT-IR data confirm that oxygen and nitrogen atoms can function as active sites in adsorption. The findings reveal that CDHBHZ is adsorbed on the MS surface.

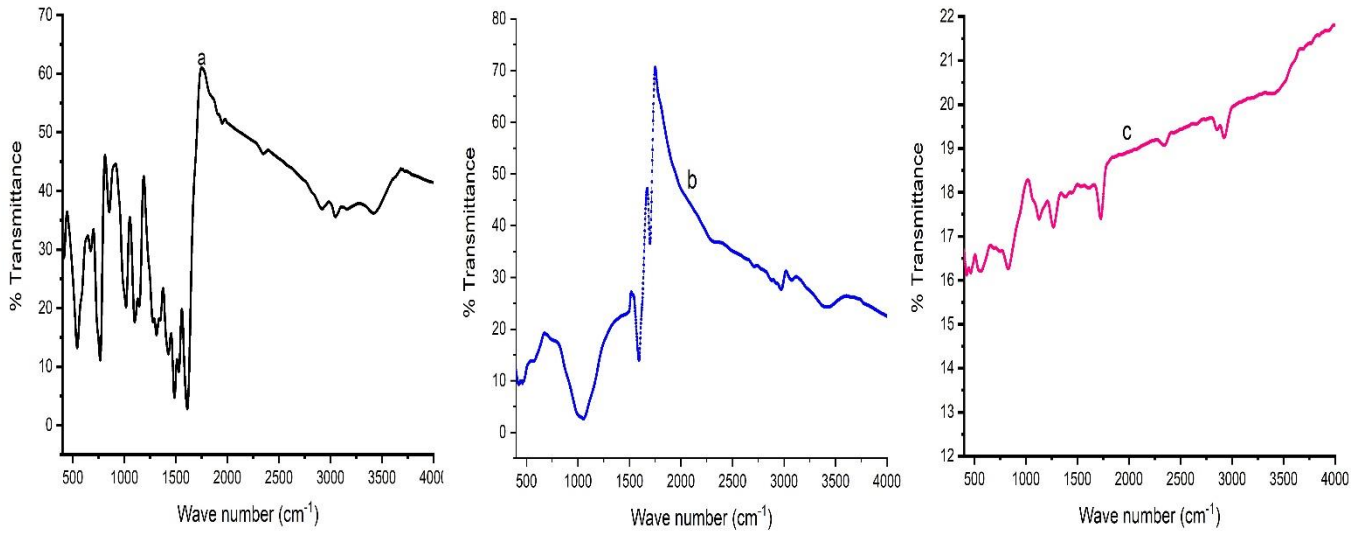

Figure 9. IR spectra of a) CDHBHZ b) The obtained surface film from MS in HCl with CDHBHZ c) The obtained surface film from MS in H_2SO_4 with CDHBHZ.

3.6. SEM Studies

Surface pictures of MS in inhibited and acid solutions are depicted in Fig.10a-d. Cavities and depth roughness were detected when MS was immersed in both solution (HCl 1M and H_2SO_4 0.5M) as illustrated in Fig.10a & c, where the surface is strongly corroded due to attack of aggressive acids. On the other hand, Fig.10b and d show that the addition of CDHBHZ reduces the depth roughness and cavities formation on the MS surface in both acid solution.

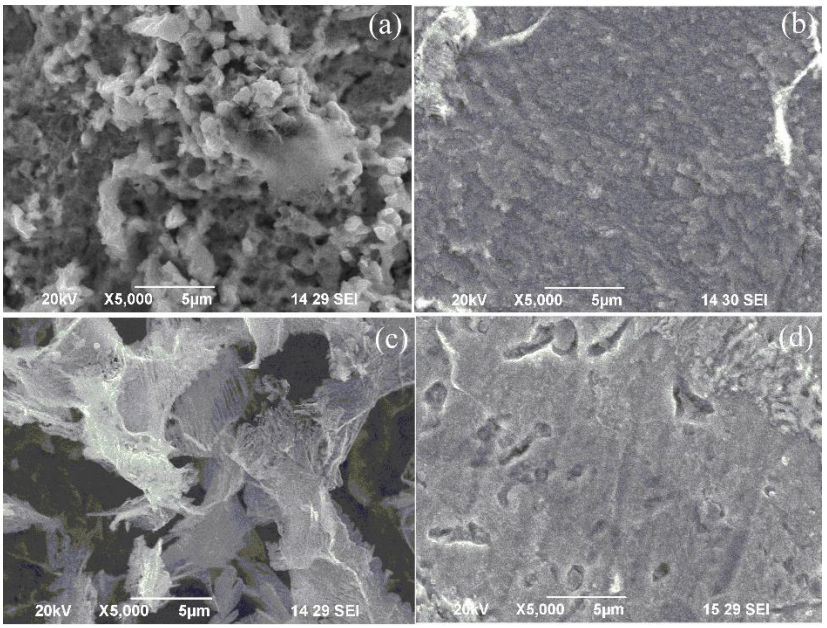

Figure 10. Morphology of MS in HCl(a), MS in HCl with 0.03M CDHBHZ (b), MS in H_2SO_4 (c), MS in H_2SO_4 with 0.03M CDHBHZ (d)

The appearance of mild steel specimens had smoothed due to CDHBHZ effect in HCl and H_2SO_4 solution. CDHBHZ acts as a mixed inhibitors inhibit both evolution of hydrogen gas and metal dissolution leading to the existence of protective layer on the MS surface. The formed active layer protects the MS surface from corroding agents.

3.7. Mechanism of Corrosion Inhibition

In general, the effectiveness of an inhibitor protection is assessed by its adsorption on a metal surface. The adsorption process is influenced by metal's composition, nature of the solution, concentration of inhibitor, temperature, pH, inhibitor chemical structure and charged surface and its distribution across inhibitor molecule.

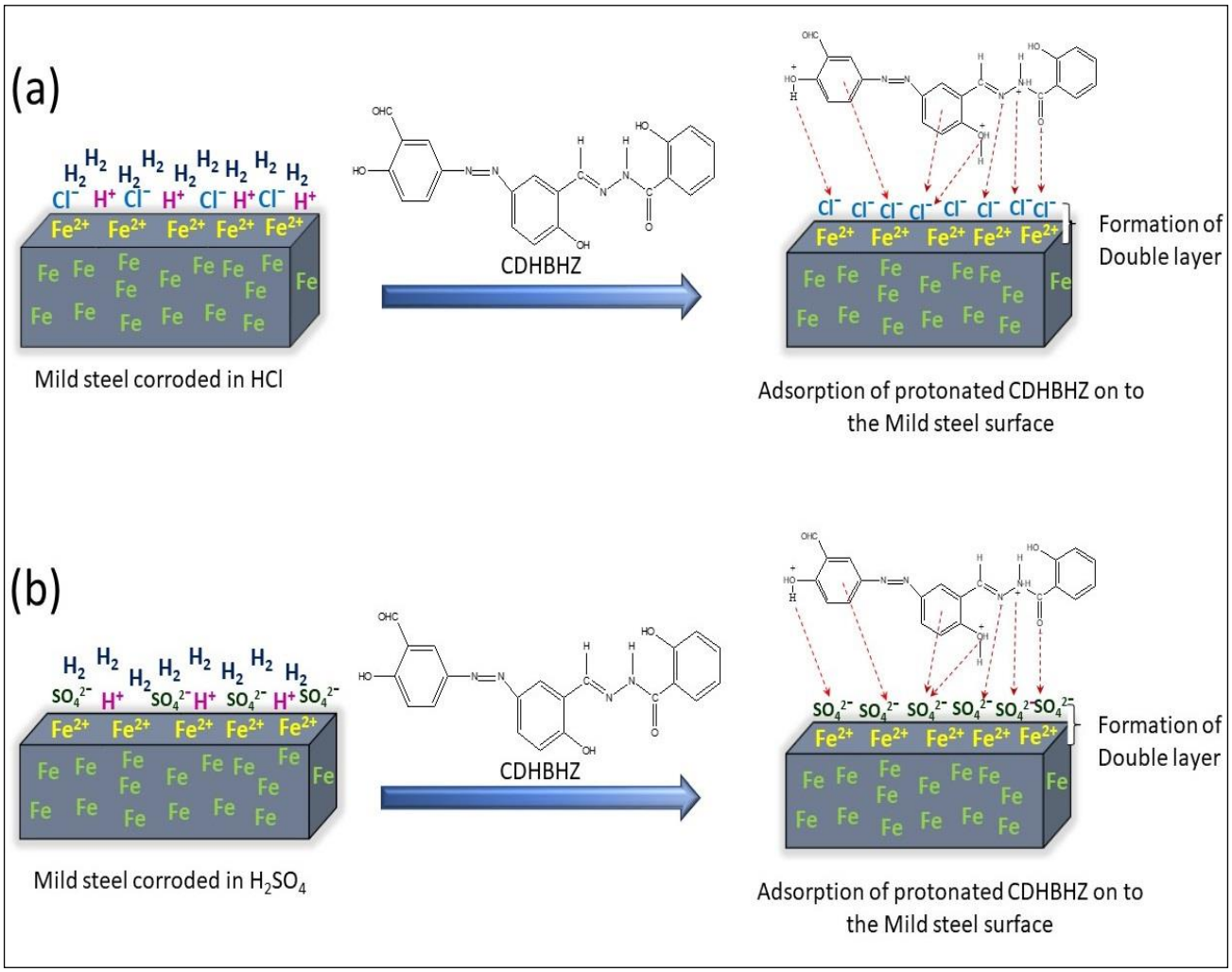

Figure 11. Schematic diagram to depict the adsorption of CDHBHZ on Fe surface in HCl (a) and H_2SO_4 (b)

Adsorption of inhibitor on the metal surfaces could be carried out in various ways [52] such as

(a) During the process of electrostatic interaction that takes place between the charged metal and the molecules that are also charged.

(b) When the non-bonding electron pairs in the molecule interact with the metal.

(c) At the time when π-electrons interact with the metal (or)

(d) When different types (a-c) combine.

The adsorption and inhibitory effect of CDHBHZ in HCl and H_2SO_4 solution can be explained as follows, based on experimental and theoretical data. In acidic aqueous solutions, CDHBHZ that has been protonated is a kind of CDHBHZ. Having neutral species adsorbed in all possible areas on the free surface sites, the surface concentration of anions would limit the cationic species adsorption in case SO_4^{2-} and Cl^- anions are adsorbed first on the metal.

It results in the CDHBHZ adsorption through van der Waals interaction taking place between the protonated CDHBHZ molecules and the metal surface that is negatively charged. And it is noted that the nature of anions could influence the adsorption of CDHBHZ. Possessing a smaller degree of hydration like chloride ions, specific adsorption of anions is expected to be more pronounced. Having been adsorbed specifically, an excess negative charge towards the solution is created which favour more adsorption of the cations. And it is probable that if the interference by sulfate ions is less it may result in lower adsorption and inhibition of corrosion. Taking into consideration all of these possibilities, we created a schematic model of the CDHBHZ adsorption processes on the mild steel surface (Fig.11).

4. CONCLUSION

Non-electrochemical and Electrochemical techniques were used to examine the inhibitive effects of CDHBHZ on MS in HCl (1M) and H_2SO_4 (0.5M). The results of the experimental study manifests that at 0.03M concentration, maximal protection efficiency for CDHBHZ approaches 96.00 % in 1M HCl and 89.00% in 0.5M H_2SO_4. It is obvious that the protection efficacy enhances as the CDHBHZ concentration increases but declines with enhance in temperature. The values of ΔH^* and E_a increase when CDHBHZ is added to the solution, showing that the energy barrier of corrosion reaction is enhanced due to inhibitive effect of CDHBHZ. The adsorption of CDHBHZ obeys Langmuir model and obtained the ΔG_{ads} values revealed that mixed mode of adsorption between CDHBHZ molecules and the mild steel surface. CDHBHZ is a comprehensive inhibitor, blocking both metal dissolution and hydrogen evolution processes, according to Potentiodynamic Polarization plots. The addition of CDHBHZ increases mild steel corrosion resistance while lowers double layer capacitance, as evidenced by AC impedance curves. The results of the functional group and surface analysis show that CDHBHZ forms an effective protective screen on the MS surface against the acid attack.

References

1. A.K. Singh, S.K. Shukla and E.E. Ebenso*, Int. J. Electrochem.Sci*., 6 (2011) 5689
2. P. Muthukrishnan, B. Jeyaprabha, P.T harmaraj and P. Prakash, *Res. Chem. Intermed*., 41 (2015) 596.
3. Y. El Kacimi, R. Touir, K. Alaoui, S. Kaya, A.S. Abousalem, M. Ouakki and M. Ebn Touhami, *J Bio Tribo Corros*., 47 (2020) 1.

4. E. Ech-chihbi, A. Nahlé, R. Salim, F. Benhiba, A. Moussaif, F. ElHajjaji, H. Oudda, A. Guenbour, M. Taleb, I. Warad and A Zarrouk, *J Alloys Compd*., 844 (2020) 155842.
5. M. Yadav, D. Behera and S. Kumar, *Surf Interface Anal*., 46 (2014) 640.
6. R. Sasi kumar, R. Karthik, S.M. Chen, P. Prakash, P. Muthukrishnan, K. Shankar and A. Kathiresan, *Int. J. Electrochem. Sci*., 11 (2016) 8892
7. J.G.N. Thomas, In; Proc 4th European Symposium on Corrosion Inhibitors, Ann Univ Ferrara N S., Sez. V.Suppl.No.7. 0879. pp 453.
8. G. Schmitt, *Br.Corros.J*., 19 (1984) 165.
9. S. Siddagangappa, S.M. Mayanna and F. Pushpanadan, *Anti-Corros Methods Mater*., 23 (1976) 11.
10. S. Sankarapapavinasam, F. Pushpanaden and M. F. Ahmed, *Br.Corros.J*., 24 (1989) 39.
11. C. Anitha, S. Sumathi, P. Tharmaraj and C.D. Sheela, *Int.J.Inorg.chem*., 2011 (2011) 1.
12. S. Deng, X.Li, *Corros. Sci*., 525 (2012) 407.
13. D. Daoud, T. Douadi, S. Issaadi and S. Chafaa, *Corros. Sci*., 79 (2014) 50.
14. S.A. Soliman, M.S. Metwally, S.R. Selim, M.A. Bedair and M.A. Abbas, *J Ind Eng Chem*., 20 (2014) 4311.
15. R. Menaka and S. Subhashini, *J Adhes Sci Tech*., 30 (2016) 1622
16. S.D. Toliwal, J. Kalpesh and T. Pavagadhi, *J Appl.Chem.,* 12 (2010) 24.
17. Y. Abboud, A. Abourriche, T. Saffaj, M. Berrada, M. Charrouf, A. Bennamara and H. Hannache, *Desalination*., 237 (2009) 175.
18. A. Saady, E. Ech-chihbi, F. El-Hajjaji, F. Benhiba, A. Zarrouk, Y. Kandri Rodi, M.Taleb, A. El Biache and Z. Rais, *J Appl Electrochem*., 51 (2021) 245.
19. A. Popova, E. Sokolova, S. Raicheva and M. Christov, *Corr Sci*., 45 (2003) 33.
20. P.M. Krishnegowda, V.T. Venkatesha, P.K.M. Krishnegowda and S.B. Shivayogiraju, *Ind.Eng.Chem.Res*., 52 (2013) 722.
21. L. Elkadi, B. Mernari, M. Traisnel, F. Bentiss and M. Lagrenee, *Corros. Sci*., 42 (2000) 703.
22. T.Y. Soror and M.A. El-Ziady, *Mater.Chem.Phys*., 77 (2002) 697.
23. M.A. Quaraishi and D. Jamal, *Mater.Chem.Phys*., 78 (2003) 608.
24. E.A. Noor, *Int.J.Electrochem.Sci*., 2 (2007) 996.
25. D.K. Singh, S. Kumar, G. Udayabhanu and R.P. John, *J Mol liq.*, 216 (2016) 738.
26. N.O. Obi-Egbedi and I.B. Obot, *Arabian J. Chem*., 5 (2010) 121.
27. L. Vracar and D.M. Drazic, *Corros. Sci*., 44 (2002) 1669.
28. Y. Tang, F. Zhang, S. Huc, Z. Cao, Z. Wu and W. Jing, *Corros. Sci*., 74 (2013) 271.
29. Z. Tao, S. Zhang, W. Li and B. Hou, *Corros.Sci*., 51 (2009) 2588.
30. A.S. Fouda, A.A. Al-Sarawy and E.E. El-Katori, *Desalination*., 201 (2006) 1.
31. M. Boukalah, B. Hammouti, M. Lagrenee and F. Bentiss, *Corros Sci*., 48 (2006) 2831.
32. D. Ozkir, K. Kayakirilmaz, E. Bayol, A.A. Gurten and F. Kandemirli, *Corros.Sci*., 56 (2012) 143.
33. P. Muthukrishnan, P. Prakash, K. Shankar, A. Kathiresan, *J Bio Tribo Corros*., 5 (2019) 1.
34. M. Muralisankar, R. Sreedharan, S. Sujith, N.S.P. Bhuvanesh and A. Sreekanth, *J. Alloys Compd*., 695 (2017) 171.
35. X. Li and G. Mu, *Appl Surf Sci*., 252 (2005) 1254.
36. G. Mu, X. Li and G. Liu, *Corros.Sci*., 47 (2005) 1932.
37. K. Tebbji, I. Bouabdellah, A. Aouniti, B. Hammouti, H. Oudda, M. Benkaddour and A. Ramdani *Mater.Lett*., 61 (2007) 799.
38. P. Mourya, S. Banerjee, R.B. Rastogi, M.M. Singh, *Ind.Eng.Chem.Res.,* 52 (2013) 12733.
39. K. Ansari, M. Quraishi and A. Singh, *Corros Sci*., 79 (2014) 5.
40. N.Z. Nor Hashima, E.H. Anouarb, K. Kassimc, H.M. Zakic, A.I. Alharthib and Z. Embonge, *Appl. Surf. Sci*., 476 (2019) 861.
41. B.M. Mıstry, N.S. Patel, S. Sahoo and S. Jauhar, *Bull. Mater. Sci*., 35 (2012) 459.
42. A. Majjane, D. Rair, A. Chahine, M. Et-tabirou, M. Ebn Touhami and R. Touir, *Corros. Sci*., 60 (2012) 98.

43. N.K. Gupta, C. Verma, M.A. Quraishi and A.K. Mukherjee, *J Mol Liq*., 215 (2016) 47
44. M.P. Chakravarthy, K.N. Mohana and C.B. Pradeep Kumar, *Int J Ind Chem.*, 5 (2014) 1
45. K.C. Emregul, A.A. Akay and O. Atakol, *Mater Chem Phys*., 93 (2005) 325.
46. K. Muthamma, P. Kumari, M. Lavanya and S.A. Rao, *J Bio Tribo Corros*., 7 (2021) 1.
47. D. K. Lavanya, Frank V. Priya and D. P. Vijaya, *J Fail. Anal. and Preven*., 20 (2020)494
48. B. M. Prasanna, B. M. Praveen, Narayana Hebbar, T. V. Venkatesha and H. C.Tandon, *Int J Ind Chem.*, 7 (2016) 9.
49. M.J. Banera, J.A. Caram, C.A. Gervasi and M.V. Mirı´fico, *J Appl Electrochem.*, 44 (2014) 1337.
50. S. Sathiyanarayanan, C. Marikkannu and N. Palaniswamy, *Appl Surf Sci*., 241 (2005) 477.
51. K.F. Khaled, *Appl. Surf. Sci*., 252 (2006) 4120.
52. D.P. Schweinsberg, G.A. George, A.K. Nanayakkara and D.A.Steiner, *Corros.Sci*., 28(1988) 33**.**